OFFICE OF NAVAL RESEARCH

Contract N00014-94-1-0323

R&T Code 413v001

Technical Report No. 2

THE ROLE OF SOLVENT DIPOLE STRUCTURE ON THE CAPACITANCE ON CHARGED INTERFACES

by

Xiaoping Gao and Henry S. White

Submitted for publication

Journal of Electroanalytical Chemistry

University of Utah
Department of Chemistry
Salt Lake City, UT 84112

April 31, 1995

REPORT DOCUMENTATION PAGE

Form Approved
OMB No. 0704-0188

1. AGENCY USE ONLY (Leave blank)	2. REPORT DATE	3. REPORT TYPE AND DATES COVERED
	3/31/95	Interim 6/94 - 12/94

4. TITLE AND SUBTITLE

The Role of Solvent Dipole Strucutre on the Capacitance of Charged Interfaces

5. FUNDING NUMBERS

N0014-94-1-0323

R & T Code 413V001

6. AUTHOR(S)

Xiaoping Gao and Henry S. White

7. PERFORMING ORGANIZATION NAME(S) AND ADDRESS(ES)

Department of Chemistry
Henry Eyring Building
University of Utah
Salt Lake City, Utah 84112

8. PERFORMING ORGANIZATION REPORT NUMBER

2

9. SPONSORING/MONITORING AGENCY NAME(S) AND ADDRESS(ES)

Office of Naval Research
800 North Quincy Street
Arlington, Virginia

10. SPONSORING/MONITORING AGENCY REPORT NUMBER

11. SUPPLEMENTARY NOTES

12a. DISTRIBUTION/AVAILABILITY STATEMENT

Unclassified/Unlimited

12b. DISTRIBUTION CODE

13. ABSTRACT (Maximum 200 words)

An electrostatic model of solvent (H_2O) dipole interactions at charged interfaces is reported. The model of H_2O used in the present study has an internal dipole structure characterized by both a dipole moment (μ_D) and a finite dipole length (d_μ). The electric force acting on an individual molecule in the first monolayer is computed as a function of d_μ, taking into account both surface charge/dipole and dipole/dipole interactions. Inclusion of the finite dimensions of the dipole and hard-core solvent diameter allows a simple and self-consistent method for calculating the interaction between solvent molecules. The capacitance of the charged interface, based on a simplistic two-state model of H_2O orientation, is shown to be sensitive to the dipole structural parameters μ_D and d_μ, demonstrating the necessity of accounting for the charge distribution within the solvent molecule. The results are discussed in terms of existing models of H_2O currently used in molecular dynamics and Monte Carlo simulations of interfacial fluid structure.

14. SUBJECT TERMS

15. NUMBER OF PAGES

16. PRICE CODE

17. SECURITY CLASSIFICATION OF REPORT	18. SECURITY CLASSIFICATION OF THIS PAGE	19. SECURITY CLASSIFICATION OF ABSTRACT	20. LIMITATION OF ABSTRACT
Unclassified	Unclassified	Unclassified	

THE ROLE OF SOLVENT DIPOLE STRUCTURE ON THE CAPACITANCE OF CHARGED INTERFACES

Xiaoping Gao and Henry S. White*
Department of Chemistry, Henry Eyring Building, University of Utah,
Salt Lake City, UT 84112

Abstract: An electrostatic model of solvent (H_2O) dipole interactions at charged interfaces is reported. The model of H_2O used in the present study has an internal dipole structure characterized by both a dipole moment (μ_D) and a finite dipole length (d_μ). The electric force acting on an individual molecule in the first monolayer is computed as a function of d_μ, taking into account both surface charge/dipole and dipole/dipole interactions. Inclusion of the finite dimensions of the dipole and hard-core solvent diameter allows a simple and self-consistent method for calculating the interaction between solvent molecules. The capacitance of the charged interface, based on a simplistic two-state model of H_2O orientation, is shown to be sensitive to the dipole structural parameters μ_D and d_μ, demonstrating the necessity of accounting for the charge distribution within the solvent molecule. The results are discussed in terms of existing models of H_2O currently used in molecular dynamics and Monte Carlo simulations of interfacial fluid structure.

Submitted to *J. Electroanal. Chem.*, September, 1994
Revised, January, 1995

Introduction. Solvent orientation at the electrode/electrolyte interface has been the subject of intense research since the first two-state dipole model of a H_2O monolayer was proposed by Watts-Tobin in 1961.[1] In the Watts-Tobin model, solvent molecules in the first monolayer of electrolyte are assumed to orient with their dipoles pointed either towards or away from the electrode surface in response to the applied electric field. At potentials far from the potential of zero charge (p.z.c.), the electric force acting on the dipole layer is sufficiently large that orientation of the dipoles is predicted to occur. Near the p.z.c., the electrostatic interaction is small compared to thermal energies, reducing the degree of dipole orientation. A key result of the Watts-Tobin model is the prediction of a maximum in the inner layer capacitance as a function of the potential. The inner layer capacitance maximum or "hump" is experimentally observed for Hg electrodes in aqueous[2] and nonaqueous[3] electrolytes, as well as for oriented solid electrodes (e.g., Ag[4-6] and Au[7-9]). In situ infrared spectroscopy of surface H_2O supports the notion of a potential-dependent solvent reorientation but also demonstrates that the solvent structure is clearly more complex than suggested by the classical two-state model.[10]

Numerous improvements and modifications of the Watts-Tobin model have been made over the course of the past 3 decades, motivated by the desire to quantitatively describe the potential-dependent capacitance and surface entropy of Hg electrodes in aqueous and non-aqueous electrolyte. Three-state[11] and multi-state models[12,13] have been introduced, and the role of hydrogen bonding[14], image charges[15], solvent tilt angle[1], solvent clustering[16,17], and higher-order polarization have been investigated. Lateral interactions between adjacent H_2O dipoles, apparently first considered by Levine et al.[15] in context of the Watts-Tobin model, have been extensively investigated by Fawcett[11,12,18] and Lamperski[19] in point-dipole models. A detailed account of progress in this field is described in a review by Guidelli.[20]

Although the above-mentioned analytical models have been remarkably successful in computing the inner layer capacitance, general objections have been raised in the

literature concerning this approach to modeling the interface.[21,22] First, the separation of the interface into an inner layer and outer layer is clearly only approximate, requiring a artificial boundary to demarcate the region in space where the solvent structure is no longer influenced by the presence of the surface. Second, the analytical models have relied on the use of point dipoles imbedded in a continuum dielectric to describe the structure of the solvent. The use of a point dipole model appears valid only when the interaction distances being considered are much larger than the actual separation of charge within the solvent molecule. This limiting case may not strictly apply to densely-packed H_2O molecules within the inner layer.

Beginning with investigations in the early 1980's, Monte Carlo (MC) and molecular dynamics (MD) simulations have been used with increasing frequency to characterize the structure of liquids at hard surfaces. The use of so-called "realistic" models of H_2O[23-27], such as the popular ST2[28] and SPC[29] models, and the avoidance of separating the double layer into inner and outer regions, suggests that the MC and MD methods offer significant advantages over the analytical approach initiated by Watts-Tobin. Indeed, fundamental insight into various electrochemical phenomena such as ion adsorption[30,31,32] and solvent dynamics[33-35] have been obtained during the past few years using realistic H_2O models in computer simulations. As with the previous analytical theories, the success of the MD and MC simulations in accurately describing interfacial properties relies to a large extent on the model of H_2O chosen for the simulation. The majority of these models are characterized by (i) a fixed-site distribution of point charges (either 3 or 4-site charge models are employed) intended to mimic the dipole and quadrupole moments of individual H_2O molecule, and (ii) a Lennard-Jones term describing the interaction between oxygen atoms of different molecules. The L-J potential is radial symmetric, allowing an effective hard-core collision diameter, σ_{LJ}, to be defined for the molecule. In the present context, it is important to note that the parameters associated with both (i) and (ii) have been determined empirically using data for *bulk* H_2O. Thus,

there is no a prior reason to assume that such H_2O models are equally well suited for simulations of interfacial H_2O. Table I lists some of the more popular models of H_2O, all of which yield reasonable properties of bulk properties of H_2O when employed in simulations (the older Rowlison model of H_2O is not currently used but is included here in order to give an example of a model based on the dielectric properties of vapor phase H_2O). Table I also lists the dipole moment (μ_D), dipole length (d_μ), and σ_{LJ} for each model. In addition, the dipole position relative to oxygen atom, and the ratio of the dipole length to the hard-core diameter (d_μ/σ_{LJ}), are schematically shown in the last column of Table I. (The reader should note that d_μ and the dipole position are not explicitly given in the original papers describing these models, but can be readily deduced from the geometrical positions of the point charges defining the model.) The interesting feature of the data in Table I is the large variance in both d_μ and the dipole position for the various H_2O models currently used in MD and MC simulations. For instance, d_μ for the BNS (1.16 Å) and ST2 (1.04 Å) models are approximately twice as large as that for SPC/E (0.58 Å) and TIPS2 (0.44 Å); on the other hand, the dipoles of BNS and ST2 H_2O are nearly symmetrically centered about the oxygen atom, while the negative end of the dipole for SPE/C and TIPS2 H_2O are positioned directly on the oxygen atom. TIP4P and PPC have relatively small values of d_μ (similar to SPC/E and TIPS2), but have symmetrically centered dipoles (similar to BNS and TIPS2). Given the dissimilarity of the dipole structures of these models, it seems unlikely that each can capture the properties of charged interfaces with equal success, since the potential distribution should depend markedly on the dipole structure of the solvent model. Indeed, a MD simulation of the capacitance of a charged Pt/H_2O interface using BJH and TIP4P models of H_2O has been reported;[36] however, this simulation failed to reproduce the potential dependence of the capacitance associated with solvent reorientation.

In this short communication, we develop a simplistic 2-state model of solvent orientation (similar to the original Watts-Tobin model) that takes into account the finite

dipole length of H_2O. The goal is to gain insight into the nature of the dependence of the interfacial capacitance on the assumed dipole structure of the solvent molecule; no attempt is made to develop a realistic picture of the interface. H_2O is modeled as a hard sphere with an imbedded dipole of finite length. Using an classical electrostatic approach recently developed for computing the potential distribution across self-assembled monolayers containing fixed site acid/base or redox centers,[37-39] we compute the inner layer and total capacitance of an ideal electrode immersed in an ideal non-adsorbing electrolyte. The results clearly demonstrate that the potential distribution and capacitance are strong functions of the dipole structure.

Results and Discussion

Model of Inner Layer Structure

Fig. 1 shows the electrostatic model used to compute the interfacial potential and charge distributions. In the monolayer adjacent to the electrode surface, solvent molecules are modeled as hard spheres of radius r_o containing an imbedded dipole. The dipole is characterized by two point charges, z_μ and $-z_\mu$, separated by a distance d_μ and symmetrically centered within the hard sphere. The dipole moment is defined as $\mu_D = z_\mu d_\mu$. A dielectric constant ε_∞ is assigned to the inner layer region (i.e., $0 < d < 2r_o$). At distances $> 2r_o$, the electrolyte solution is assumed to be a structureless fluid with a potential distribution governed by the Gouy-Chapman model, decaying to ϕ_s in the bulk. The solution contains a symmetrical z:z electrolyte and is assigned a dielectric constant ε_s.

The average electric field E at the center of the monolayer can be calculated as the sum of the electric fields contributed from the metal surface (E_m) and from the dipoles (E_d):

$$E_T = E_m + E_d = \frac{\sigma_m}{\varepsilon_o \varepsilon_\infty} + \frac{\sigma_1}{\varepsilon_o \varepsilon_\infty} \qquad (1)$$

In eq. 1, σ_m is the average charge density on the metal surface and ε_0 is the permittivity of vacuum. The quantity σ_1 is the charge density on the plane defined by the end of the dipole nearest the electrode surface (Fig. 1), and is given by

$$\sigma_1 = z_\mu F(\Gamma_1 - \Gamma_2) \tag{2}$$

where Γ_1 and Γ_2 are the surface concentrations (mol/cm^2) of solvent molecules having their dipoles directed towards or away from the electrode, respectively. Similarly, σ_2 is defined as the charge density of the plane defined by the end of the dipole furthest from the surface. By definition, $\sigma_1 = -\sigma_2$.

Using eq. (2), the electric field across the inner layer can be thus be written in terms of the parameters μ_D and d_μ.

$$E_T = \frac{\sigma_m}{\varepsilon_o \varepsilon_\infty} + \frac{\mu_D F(\Gamma_1 - \Gamma_2)}{d_\mu \varepsilon_o \varepsilon_\infty} \tag{3}$$

Unlike results obtained using point-dipole models of the inner layer, eq. 3 indicates clearly shows that the electric force acting on a solvent molecule is expected to be a function of the charge distribution within the molecule.

Levine et al.[15] and Fawcett and coworkers[11,12,18] have previously demonstrated the importance of taking into account lateral electrostatic interactions between neighboring dipoles. Their approach to computing the dipole-dipole interaction is based on a two-dimensional hexagonal lattice model. Assuming a point dipole solvent molecule, the field acting on a central dipole, due the dipole field of the neighboring solvent molecules is given by

$$E_d^{eff} = \frac{C}{d_3}\left(m_p + m_i\right)$$

where C is a coordination number, d is distance between nearest neighbors, and m_p and m_i are the average permanent and induced dipole moments per site (for instance, $m_p = (\Gamma_1 - \Gamma_2)\mu_D / \Gamma_T$). The precise value of C critically depends on how dipole-dipole and dipole images are computed, as has been previously discussed in detailed in the literature.[40-42] The lattice approach ignores local equilibrium between neighboring dipoles; i.e, the probablility of a neighboring dipole being in an up or down configuration is independent of the orientiational state of the central dipole (and vice versa). This "random approximation"[15] leads to a value of E_d^{eff} that is the same at all dipole sites.

By analogy with the above strategy, the lateral interactions between dipoles of finite dimension d_μ can be computed by summing the field at the position of a central dipole due to the charge densities σ_1 and σ_2. Fig. 2 shows an individual dipole of length d_μ imbedded in a hard sphere of diameter $2r_o$. The planes of charge σ_1 and σ_2 are located at a distance $(1/2)d_\mu$ above and below the dipole center. The field at the center of the dipole is computed, excluding its own field, by integrating the field resulting from the charged planes between r_o and ∞:

$$E_d^{eff} = \frac{2}{4\pi\varepsilon_o\varepsilon_\infty}\int_{r_0}^{\infty}\frac{(d_\mu/2)\sigma_1 2\pi r}{[(d_\mu/2)^2 + r^2]^{3/2}}dr$$

$$= \frac{\sigma_1}{\varepsilon_o\varepsilon_\infty}\frac{d_\mu/2}{[(d_\mu/2)^2 + r_0{}^2]^{1/2}} \qquad (4)$$

$$= \lambda E_d$$

where $\lambda = \frac{d_\mu/2}{[(d_\mu/2)^2 + r_o{}^2]^{1/2}}$. Similar to the use of an average dipole moment (m_p) in the point dipole models, the use of averaged charge densities (σ_1 and σ_2) is based on the

approximation of random dipole orientation (no nearest neighbor correlation). The use of averaged charge densities, rather than discrete charges on a lattice sites, however, allows for a simple method of computing long-range electrostatic interactions.

From eq. (4), the lateral interaction is determined by λ, which in turn, is a function of μ_D and the solvent radius r_o. Using the terminology of Damaskin[17], λ may be referred to as a discreteness coefficient that accounts (albeit approximately) for the finite dimensions of both the solvent and dipole length.

It is readily seen from eq. (4) that when λ is equal to 1, $E_d^{eff} = E_d$. Physically, this corresponds to including the dipole self-interaction in computing the force acting on the dipole (as assumed by Watts-Tobin[1]). On the other hand, λ equal to 0 corresponds to neglecting the lateral interactions (i.e., $E_d^{eff} = 0$, as assumed in several theories). Clearly, λ should take on a value between 0 and 1. For the so-called realistic H_2O models listed in Table 1, λ has values ranging from 0.15 (TIPS2) to 0.38 (BNS) (approximating $2r_o$ by σ_{LJ} and ignoring the offset of the dipole from the central oxygen atom position). In the following sections, λ and E_d^{eff} (eq. 4) are used to compute the total electric field, E_T (eq. 1), acting on a dipole in the inner layer.

The potential drop across the inner layer is given by:

$$\Delta\phi_i = \phi_m - \phi_{2r_o} = \frac{2r_o\sigma_m}{\varepsilon_o\varepsilon_\infty} + \frac{\sigma_1 d_\mu}{\varepsilon_o\varepsilon_\infty}$$

$$= \frac{2r_o\sigma_m}{\varepsilon_o\varepsilon_\infty} + \frac{\mu_D F(\Gamma_1 - \Gamma_{2)}}{\varepsilon_o\varepsilon_\infty} \qquad (5)$$

Unlike the electric field, the potential drop across the inner layer does not depend on the dipole structure.

As previously noted, the molecular orientation is anticipated to be a function of applied potential if the electrostatic forces between the charges on the metal and on the molecule are sufficiently large to flip the molecules between an inwards and outwards

configuration. As an approximation of the influence of electrostatic potential on the molecular orientation, we assume that the electrochemical potential of the solvent is given by

$$\bar{\mu}_j = \mu_j^o + RT \ln a_j - F(E_T \cdot \mu_D)_j \tag{6}$$

where R and T are the molar gas constant (J mol^{-1} K^{-1}), and the absolute temperature (K), respectively. The subscript j refers to the two possible dipole orientations (positive end inwards (j = 1) and outwards (j = 2) surface). At equilibrium, $\bar{\mu}_1 = \bar{\mu}_2$. Approximating the activities in eq. 6 by the respective surface concentrations Γ_1 and Γ_2, yields a relationship between the potential drop across the inner layer and the orientation of the dipoles.

$$E_T d_\mu = -\left(\frac{\mu_1^o - \mu_2^o}{2 z_D F}\right) - \frac{RT}{2 z_D F} \ln \frac{\Gamma_1}{\Gamma_2} \tag{7}$$

Eq. 7 is the same as that derived by statistical methods. The first term on the r.h.s. of eq. 7 describes the difference in the nonelectrostatic interactions between the two allowed dipole orientations. We define the fraction of molecules with positive charge oriented inwards toward the electrode surface as $f = \Gamma_1 / \Gamma_T$ (where $\Gamma_T = \Gamma_1 + \Gamma_2$), and $\xi^o = -(\mu_1^o - \mu_2^o) / 2 z_d F$. At the p.z.c., the ratio Γ_1 / Γ_2 will be determined solely by ξ^o. Substituting eq. 7 into eq. 1, replacing E_d by E_d^{eff}, and using $\Gamma_1 - \Gamma_2 = (2f - 1)\Gamma_T$, yields the charge density on metal, σ_m.

$$\sigma_m = \frac{\varepsilon_o \varepsilon_\infty}{d_\mu}\left[\xi^o + \frac{RT}{2 z_\mu F} \ln\left(\frac{1-f}{f}\right)\right] - z_\mu \lambda F (2f - 1)\Gamma_T \tag{8}$$

The inner layer capacity C_i can be obtained, using eq. 5, by differentiating the surface charge with respect to the inner layer potential $\Delta\phi_i$:

$$C_i^{-1} = \frac{\partial \Delta\phi_i}{\partial \sigma_m}$$

$$= C_1^{-1} + C_2^{-1}\frac{\partial \sigma_1}{\partial \sigma_m} \tag{9}$$

$$= C_1^{-1} - C_2^{-1}\left[\left(\frac{\varepsilon_o \varepsilon_\infty RT}{2z_\mu F d_\mu \lambda f(1-f)}\frac{\partial f}{\partial \sigma_m}\right) + \lambda^{-1}\right]$$

where $C_1 = \varepsilon_o\varepsilon_\infty / 2r_o$ and $C_2 = \varepsilon_o\varepsilon_\infty / d_\mu$. The term $\partial f/\partial\sigma_m$ is calculated from eq. 8:

$$\frac{\partial f}{\partial \sigma_m} = -\left[\frac{\varepsilon_o\varepsilon_\infty}{2}\frac{RT}{\mu_D F}\frac{1}{f(1-f)} + 2z_\mu \lambda f F \Gamma_T\right]^{-1} \tag{10}$$

The total capacity of the interface is given by:

$$C_T^{-1} = C_i^{-1} + C_{dif}^{-1}, \tag{11}$$

where $C_{dif} = \varepsilon_o\varepsilon_s\kappa\cosh\left[ze\left(\phi_{2r_o} - \phi_s\right)/2kT\right]$. The potential drop across the diffusion layer $(\phi_{2r_o} - \phi_s)$ can be evaluated by noting that the diffuse layer charge σ_{dif} is equal, but of opposite sign, to the charge density on the metal, i.e., $-\sigma_m = \sigma_{dif} = -\left(2kT\varepsilon_o\varepsilon_s\kappa/ze\right)\sinh\left[ze\left(\phi_{2r_o} - \phi_s\right)/2kT\right]$. Solving for $(\phi_{2r_o} - \phi_s)$ yields[37]

$$(\phi_{2r_o} - \phi_s) = \frac{2kT}{ze}\ln\left(\frac{ze\sigma_m}{2kT\varepsilon_o\varepsilon_s\kappa} + \left[\left(\frac{ze\sigma_m}{2kT\varepsilon_o\varepsilon_s\kappa}\right)^2 + 1\right]^{1/2}\right) \tag{12}$$

Substituting eqs. 9, 10, and 12 into eq. 11 yields the total capacitance of the electrode.

Effect of dipole length on the inner layer capacitance.

Fig. 3 shows the dependence of the inner layer capacitance as a function of the charge density on the metal and dipole length d_μ. The set of constants used in these calculations are μ_D = 1.84 D,[43] $2r_o$ = 3.2 Å,[40] and ε_∞ is 6,[17,20] corresponding roughly to expected parameters for H_2O at a metal interface. Results are shown for d_μ between 0.001 and 1.6Å, corresponding to $380 > z_\mu > 0.238e$ and $0.000313 < \lambda < 0.447$. The total dipole coverage is calculated as $\Gamma_T = (r_0^2 N_A)^{-1} = 1.7 \times 10^{-9}$ mol/cm^2, where N_A is Avogadro' number.

As can be seen in Fig. 3, the inner layer capacitance is a relatively strong function of d_μ, the maximum in C_i increasing by nearly a factor of 2 as d_μ in increased from 0.001 Å to 1.6 Å. The increase in capacitance with increasing d_μ is clearly a consequence of the closer proximity of the dipole charge to the surface, thereby inducing a larger charge on the metal.

The results in Fig. 3 show that the inner layer capacitance is essentially independent of the dipole structure for values of d_μ less than ~0.8 Å. Thus, the model developed here for a dipole of finite length reduces to that of a point dipole model when $d_\mu < \sim 0.8$ Å. A more precise statement of this limiting case is that $d_\mu/r_o << 1$. For small values of d_μ/r_o, $(d_\mu/2)^2$ can be ignored from the denominator of eq. (4), yielding $\lambda = d_\mu/2r_o$. When $\lambda = d_\mu/2r_o$ is substituted into eq. 9 for the inner layer capacitance, it is straightforward to show that the resulting equation is a function of the dipole moment μ_D, but independent of the dipole length d_μ.

In Fig. 4, the components of the electric field within the dipole layer are plotted as a function of total potential drop $(\phi_m - \phi_s)$across the inner and outer (diffuse) layers. As expected, the dipole field (either E_d or E_d^{eff}) always opposes the field due to the surface charge on the metal, E_m. However, inclusion of the dipole-dipole interactions in

computing E_d^{eff}, significantly reduces the dipole field in comparison to E_d (corresponding to $\lambda = 1$). On the over hand, E_d^{eff} is makes a significant contribution to the total field and cannot be neglected. For example, for the parameters used in computing the results in Fig. 4 (μ_D = 1.84 D, $2r_0$ = 3.2 Å, ε_∞ is 6, and d_μ = 0.5 Å), the magnitude of E_d^{eff} is always comparable to that of E_m. Thus, ignoring the dipole field (i.e., setting $\lambda = 0$) results in a significant error in the inner layer field strength.

Together, Figs. 3 and 4 clearly show that proper accounting of the lateral forces is critical in determining the interfacial charge and potential distributions. As previously noted, a number of theories have completely ignored ($\lambda = 0$) or greatly overestimated ($\lambda = 1$) dipole-dipole interactions. It is thus interesting to briefly examine the magnitude of error expected in C_i when λ is chosen in a somewhat arbitrary fashion. In Fig. 5, we show a set of inner-layer capacitance curves as a function of λ using the same set of parameters as above with d_μ = 0.5 Å, except that two of the three values of λ are chosen independently of d_μ, rather than being calculated from eq. 4. The three curves in Fig. 5 corresponding to λ = 0.120, 0.154, and = 0.180 (where $\lambda = 0.154$ corresponds exactly to d_μ = 0.5 Å as computed from eq. 4). Fig. 5 shows that the shape and magnitude of the capacitance curves are extremely sensitive to λ; less than a 0.04 variation in λ totally changes the shape of curve. The point here is that a small error in the computation of the dipole-dipole interaction is greatly amplified in the resulting capacitance curves.

Conclusion.

The results presented here demonstrate that the interfacial capacitance is a relatively strong function of the assumed dipole structure of the solvent molecule. The dependence of the capacitance on d_μ arises through lateral dipole-dipole interactions. Values of the capacitance using a simple two-state model have been shown to be independent of d_μ for $0 < d_\mu < 0.8$Å for H_2O. This finding suggests that many of the realistic models of H_2O listed in Table I, which have $d_\mu < 0.8$ (the exceptions being BNS and ST2 models),

should yield qualitatively equivalent results. However, the dipole structure is only one of several parameters used in optimizing H_2O models for MD and MC simulations. Clearly, the induced dipole polarizability, ignored in our present treatment, will be important in determining interfacial dielectric properties.

An interesting result of our investigations is that, for values of d_μ smaller than ~0.8 Å, the finite-length dipole model of H_2O yields values of the interfacial capacitance that are in quantitative agreement with results for a point-dipole structure. Even somewhat larger values of d_μ (e.g., 1 Å) yield capacitance values within 20% of the values obtained for a point-dipole structure. Thus, it follows that the earlier criticisms of using point-dipole models of H_2O (see Introduction) are not as well founded as previously suggested.

Acknowledgment. Financial support by the Office of Naval Research is gratefully acknowledged.

References.

1. R. J. Watts-Tobin, Phil. Mag., 6 (1961) 133.
2. D. C. Grahame, J. Am. Chem. Soc., 79 (1957) 2093.
3. R. Payne, Adv. Electrochem. Electrochem. Eng., 7 (1970) 1.
4. G. Valette, J. Electroanal. Chem., 269 (1989) 191.
5. G. Valette, J. Electroanal. Chem., 138 (1982) 37.
6. G. Valette, J. Electroanal. Chem., 122 (1981) 285.
7. A. Hamelin, J. Electroanal. Chem., 138 (1982) 395.
8. G. Valette and A. Hamelin, J. Electroanal. Chem., 45 (1973) 301.

9. A. Hamelin, in *Modern Aspects of Electrochemistry*, Vol. 16, B. E. Conway, R.E. White, and J. O'M. Bockris, eds., Plenum, New York, 1986, Chapter 1.

10. A. E. Russell, A. S. Lin, and W. E. O'Grady, J. Chem. Soc. Faraday Trans., 89 (1993) 195.

11. W. R. Fawcett, J. Phys. Chem., 82 (1978), 1385.

12. W. R. Fawcett and R. M. de Nobriga, J. Phys. Chem., 86 (1982) 371.

13. J. R. Macdonald and C. A. Barlow, J. Chem. Phys., 36 (1962) 3062.

14. R. Guidelli, J. Electroanal. Chem., 123 (1981) 59.

15. S. Levine, G. M. Bell, and A. L. Smith, J. Phys. Chem., 73 (1969) 3534.

16. R. Parsons, J. Electroanal. Chem., 59 (1975) 229.

17. B.B. Damaskin, J. Electroanal. Chem., 75 (1977) 359.

18. W. R. Fawcett, SA. Levine, R. M. de Nobriga, and A. C. McDonald, J. Electroanal. Chem., 111 (1980) 163.

19. S. Lamperski, J. Electroanal. Chem., 318 (1991) 39.

20. R. Guidelli, in *Trends in Interfacial Electrochemistry*, A.F. Silva, ed., Reidel, Dordrecht, Holland, 1986.

21. G. Aloisi, R. Guidelli, R. A. Jackson, S. M. Clark, and P. Barnes, J. Electroanal. Chem., 206 (1986) 131.

22. D. Henderson, in *Trends in Interfacial Electrochemistry*, A.F. Silva, ed., Reidel, Dordrecht, Holland, 1986.

23. J. S. Rowlison, Trans. Faraday Soc., 47 (1951) 120.

24. W. L. Jorgenson, J. Chem. Phys., 77 (1982) 4156.

25. P.G. Kusalik and I. M. Svishchev, Science, 265 (1994) 1219.

26. W. L. Jorgenson, J. Chandrasekhar, J. D. Madura, R. W. Impey, and M. L. Klein, J. Chem. Phys., 79 (1983) 926.

27. A. Ben-Naim and F. H. Stillinger, "Aspects of the Statistical-Mechanical Theory of Water," in *Structure and Transport Processes in Water and Aqueous Solutions*, R. A. Horne, ed., Wiley, New York, 1972.

28. F. H. Stillenger and A. Rahman, J. Chem. Phys., 60 (1974) 1545.

29. H. J. C. Berendsen, J. P. M. Postma, W. F. van Gunteren and J. Hermans, in *Intermolecular Forces*, B. Pullman, ed., Reidel, Dordrecht, Holland, 1881.

30. J. Seitz-Beywl, M. Poxleitner, and K. Heinzinger, Z. Naturforsch, 46 (1991) 876.

31. J. N. Gloshi and M. R. Philpott, J. Chem. Phys., 96 (1992) 6962.

32. E. Spohr and K. Heinzinger, J. Chem. Phys., 84 (1986) 2304.

33. K. Raghavan, K. Foster, K. Motakabbir, and M. Berkowitz, J. Chem. Phys., 94 (1991) 2110.

34. A. A. Gardner and J. P. Valleau, J. Chem. Phys., 86 (1987) 4171.

35. K. Heinzinger and E. Spohr, Electrochim. Acta., 34 (1989) 1849.

36. G. Nagy, K. Heinzinger, and E. Spohr, Farad. Discuss., 94 (1992) 307.

37. C. P. Smith and H. S. White, Anal. Chem., 64 (1992) 2398.

38. C. P. Smith and H. S. White, Langmuir, 9 (1993) 1.

39. W. R. Fawcett, M. Fedurco, and Z. Kovacova, Langmuir, 10 (1994) 2403.

40. P. Nikitas, Can. J. Chem., 64 (1986) 1286.

41. W. R. Fawcett, J. Chem. Phys., 93 (1990) 6813.

42. W. Schmickler, J. Electronanal. Chem., 149 (1983) 15.

43. D. Eisenberg, and W. Kauzmann, The Structure and Properties of Water, Oxford U. P., New York, 1969.

Figure Captions.

1. Schematic drawing of solvent molecules adjacent to an electrode surface. The solvent is modeled as hard spheres with an imbedded dipole of finite length d_μ. The potential profile is shown across the inner and diffuse layers. The ends of the solvent dipole define hypothetical planes of mean charge density (σ_1 and σ_2) and potential (ϕ_1 and ϕ_2).

2. Model system used to calculate dipole-dipole interactions within the inner layer.

3. Dependence of the inner layer capacitance as a function of the charge density on the metal (σ_m) and the dipole length (d_μ). The set of parameters used in these calculations are $\mu_D = 1.84$ D, $2r_o = 3.2$ Å, $\varepsilon_\infty = 6$. Values of d_μ are listed on the figure, and correspond to $0.000313 < \lambda < 0.447$ and $360 > z_\mu > 0.225e^-$ (see text).

4. Components of the inner layer electric field as a function of the total interfacial potential drop. E_m = field resulting from surface charge on the electrode; E_d = total dipole field ($\lambda = 1$); and E_d^{eff} = dipole field acting on an individual solvent molecule. The dashed lined corresponds to the total field acting on an individual solvent molecule ($E_T = E_m + E_d^{eff}$). The parameters used in the calculation are the same as in Fig. 3 with $d_\mu = 0.5$ Å.

5. The inner layer capacitance as a function of λ for a constant d_μ (= 0.5 Å). Values of λ used in computing the capacitance are chosen independently of d_μ to show the effect of under or overestimation of the lateral interactions. Other parameters used as the same as in Fig. 3

Table I. Dipole Parameters of Molecular Models of H_2O

Model [ref.]	μ_D(D)	d_μ (Å)	σ_{LJ} (Å)	Dipole Position
Rowlinson[23]	1.84	0.58	2.73	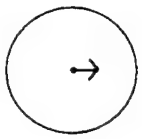
TIPS2[24]	2.24	0.44	3.24	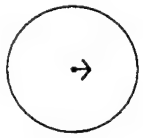
BNS[27]	2.17	1.16	2.82	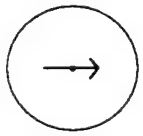
ST2[28]	2.35	1.04	3.10	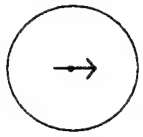
SPC/E[29]	2.35	0.58	3.17	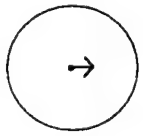
PPC[25]	2.52	0.54	3.23	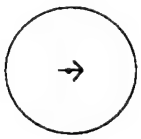
TIP4P[26]	2.18	0.55	3.15	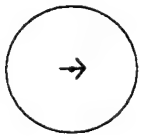

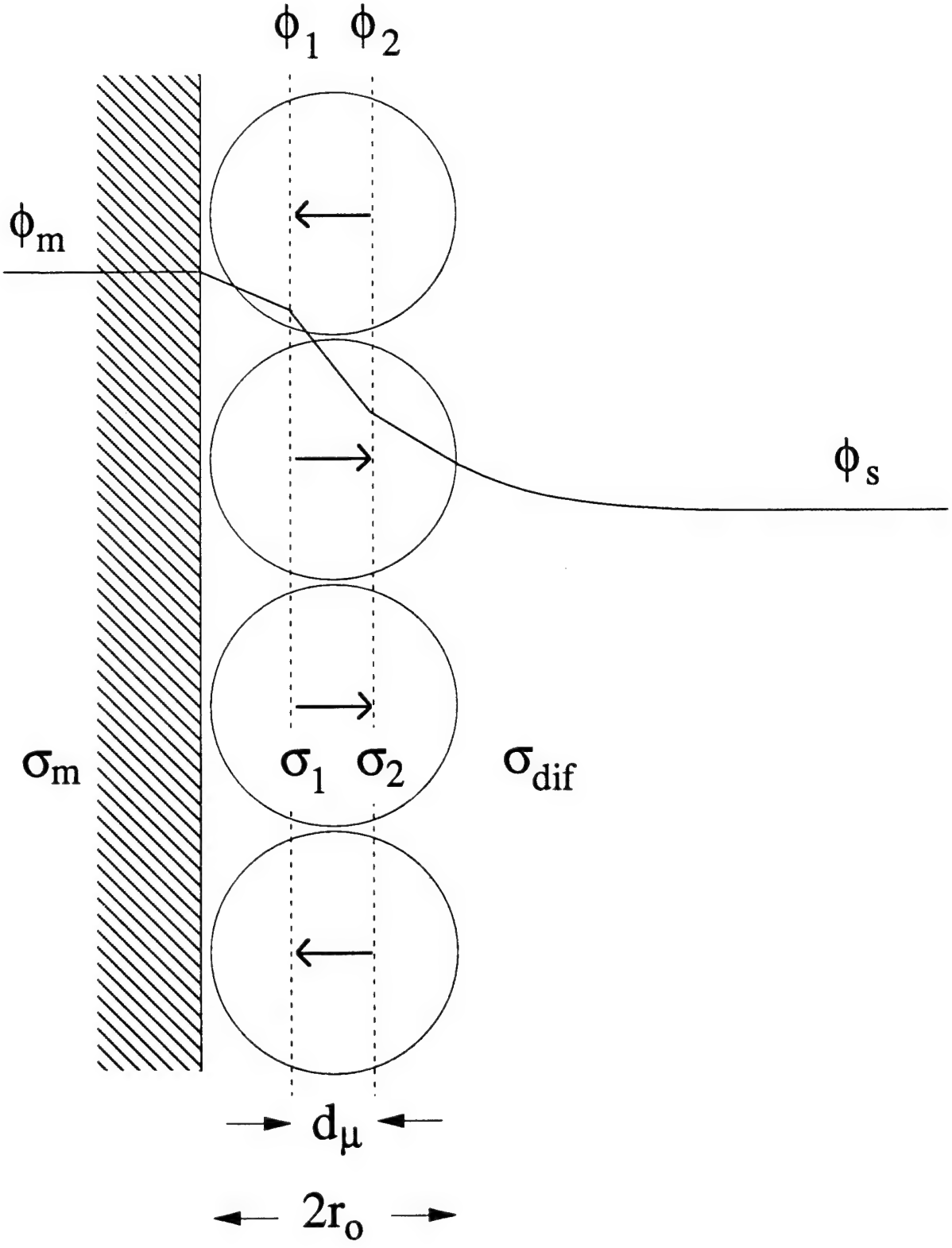

Fig 1

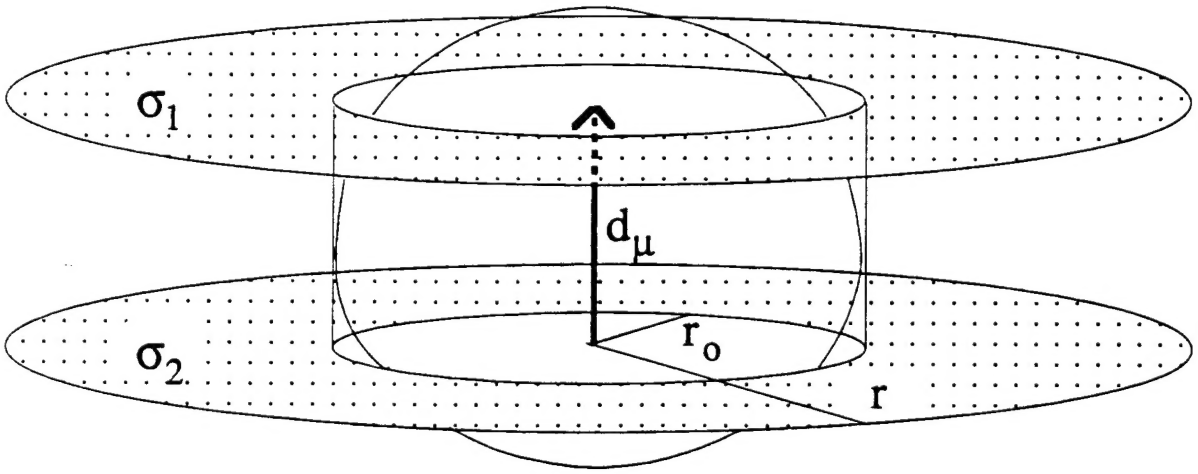

Fig. 2

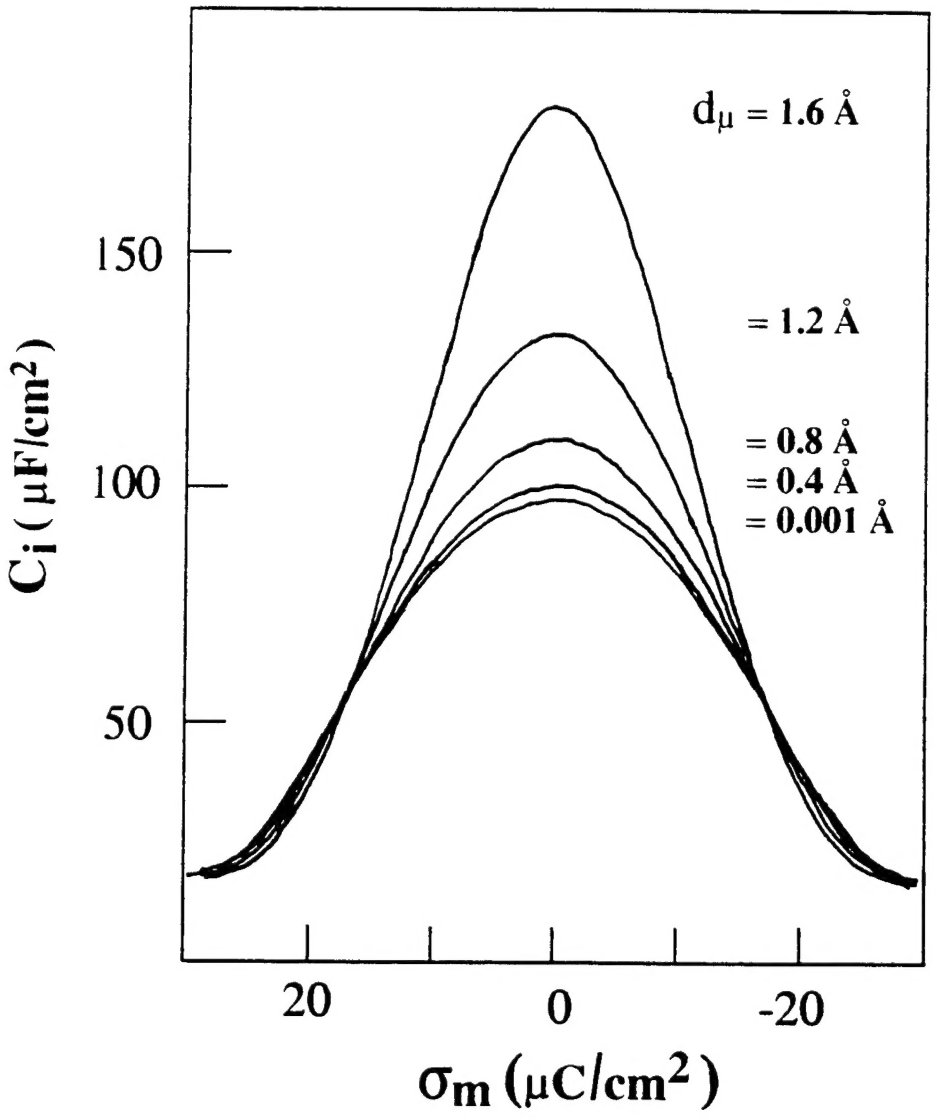
d_μ = 1.6 Å
= 1.2 Å
= 0.8 Å
= 0.4 Å
= 0.001 Å
150
100
50
C_i (μF/cm²)
20
0
-20
σ_m (μC/cm²)

Fig. 3

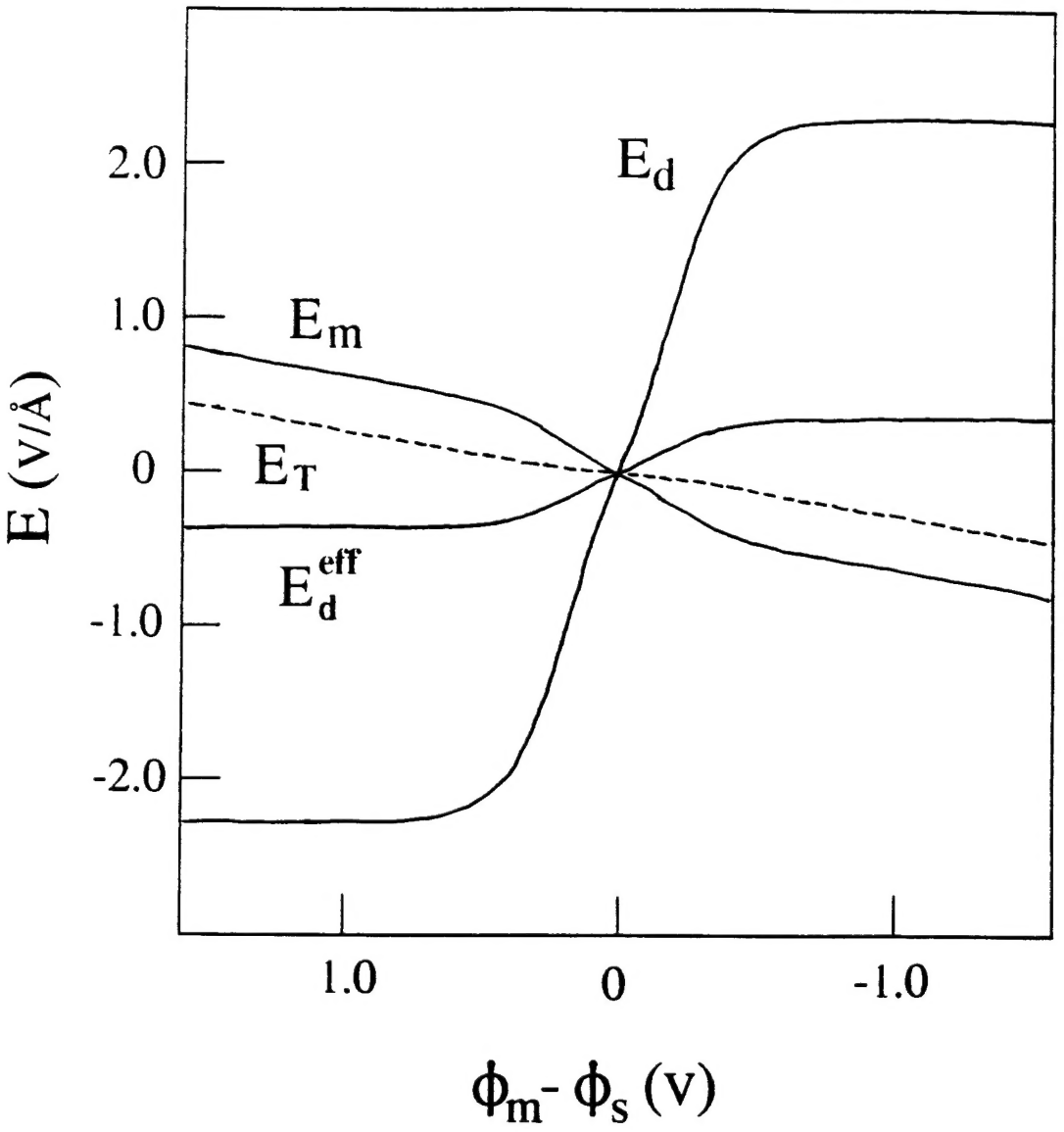

Fig 4.

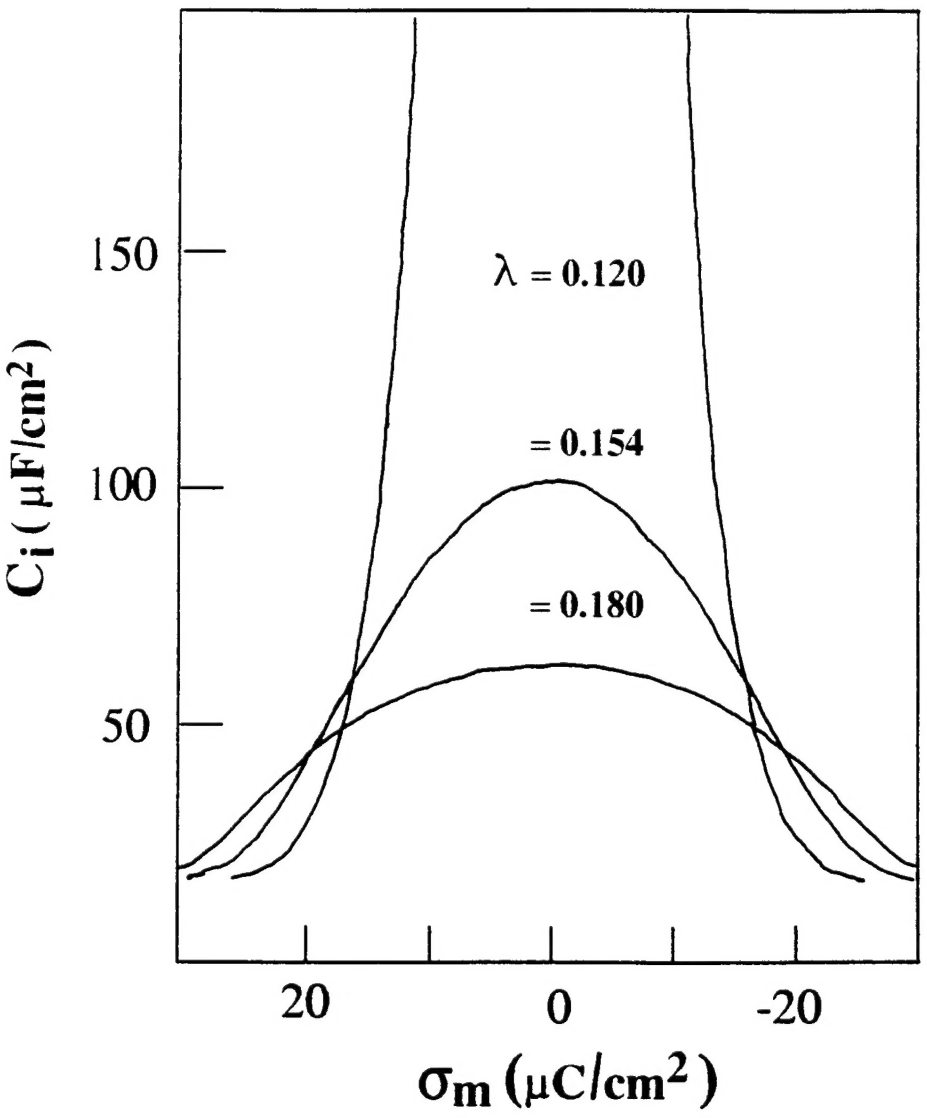
150
100
50
C_i ($\mu F/cm^2$)
λ = 0.120
= 0.154
= 0.180
20
0
-20
σ_m ($\mu C/cm^2$)

Fig. 5